Auxiliary material

Testing for a CO_2 fertilization effect on growth of Canadian boreal forests

Martin P. Girardin

Natural Resources Canada, Canadian Forest Service, Laurentian Forestry Centre, 1055 du P.E.P.S, P.O. Box 10380, Stn. Sainte-Foy, Québec, QC, G1V 4C7, Canada

Pierre Y. Bernier

Natural Resources Canada, Canadian Forest Service, Laurentian Forestry Centre, 1055 du P.E.P.S, P.O. Box 10380, Stn. Sainte-Foy, Québec, QC, G1V 4C7, Canada

Frédéric Raulier

Faculté de foresterie et de géomatique, Université Laval, Québec, QC, G1K 7P4, Canada

Jacques C. Tardif

Canada Research Chair in Dendrochronology, Centre for Forest Interdisciplinary Research (C-FIR), University of Winnipeg, 515 Portage Avenue, Winnipeg, MB, R3B 2E9 Canada

France Conciatori

Canada Research Chair in Dendrochronology, Centre for Forest Interdisciplinary Research (C-FIR), University of Winnipeg, 515 Portage Avenue, Winnipeg, MB, R3B 2E9, Canada

Xiao Jing Guo

Natural Resources Canada, Canadian Forest Service, Laurentian Forestry Centre, 1055 du P.E.P.S, P.O. Box 10380, Stn. Sainte-Foy, Québec, QC, G1V 4C7, Canada

Introduction

The purpose of this Auxiliary material is to provide some information of less central importance to the paper which cannot be included in the main body of the text because of space limitations. The Auxiliary material contains one pdf document, five figures and two tables.

Table of contents

Fig. S5 R-squared of the least-squares linear fit between 5-yr non-overlapping means of TGI and NPPAR times series (N = 17 pentads) under various simulation runs of β factors

Fig. S6 The mean of squares of the residuals (MSR) obtained after the application of different smoothing techniques of the mean growth curve, or after data truncations of the raw measurement series

Table S1 Attributes of the temporary sample plots of the DMPF Lands Inventory

Plot id.	Longitude (degrees)	Latitude (degrees)	Elevation[a] (m)	Slope (degrees)	Aspect (degrees)	Nha [b]	Wabg[c]	Soil type
188	-100.96	51.76	708	2.29	334	1200	295.1	Silty Clay
189	-100.96	51.76	708	1.72	160	500	128.5	Silty Clay
191	-100.96	51.76	708	1.72	160	500	138.6	Silty Clay
193	-100.96	51.76	693	4.57	296	1700	163.1	Silty Clay
194	-100.96	51.76	687	4.57	296	1300	217.8	Sandy Clay Loam
197	-100.96	51.76	688	11.31	271	2600	277.3	Sandy Clay
231	-100.96	51.76	703	7.41	219	1000	158.0	Silty Clay
233	-100.96	51.76	703	7.41	219	1200	145.8	Sandy Clay
321	-100.96	51.90	711	3.43	240	200	88.0	Silty Clay
396	-100.82	51.49	756	0.00	0	300	50.9	Clay Loam

[a] above sea level

[b] number of stems per hectare

[c] aboveground biomass

Table S2 Parameters and allometric coefficients used in the bioclimatic model StandLEAP

Description	Value
Plot-level partition model parameters	
Allometric coefficient *a* relating foliage biomass to crown biomass; these are the parameters of the equation $y = ax^b$, where x is the crown biomass	0.82
Allometric coefficient *b* relating foliage biomass to crown biomass; these are the parameters of the equation $y = ax^b$, where x is the crown biomass	0.93
Allometric coefficient *a* relating stem biomass to aboveground biomass; these are the parameters of the equation $y = ax^b$, where x is the crown biomass	0.60
Allometric coefficient *b* relating stem biomass to aboveground biomass; these are the parameters of the equation $y = ax^b$, where x is the crown biomass	1.03
Allometric coefficient *a* relating coarse root biomass to aboveground biomass; these are the parameters of the equation $y = ax^b$, where x is the crown biomass	1.40
Allometric coefficient *b* relating coarse root biomass to aboveground biomass; these are the parameters of the equation $y = ax^b$, where x is the crown biomass	0.79
Allometric coefficient *a* relating crown biomass to aboveground biomass; these are the parameters of the equation $y = ax^b$, where x is the crown biomass	2.01
Allometric coefficient *b* relating crown biomass to aboveground biomass; these are the parameters of the equation $y = ax^b$, where x is the crown biomass	0.76
Tree-level partition model parameters	
Allometric coefficient *a* relating aboveground biomass and DBH; these are the parameters of the equation $y = ax^b$, where x is the average DBH	0.07
Allometric coefficient *b* relating aboveground biomass and DBH; these are the parameters of the equation $y = ax^b$, where x is the average DBH	2.49
Allometric coefficient *a* relating stemsapwood biomass and DBH; these are the parameters of the equation $y = ax^b$, where x is the average DBH	0.01
Allometric coefficient *b* relating stemsapwood biomass and DBH; these are the parameters of the equation $y = ax^b$, where x is the average DBH	2.69
Fine root foliage ratio	0.68

Epsilon and water use efficiency model parameters

Parameter β_l for the epsilon temperature modifier (see eq. 3)	0.36
Parameter β_q for the epsilon temperature modifier (see eq. 3)	-0.19
Parameter $\overline{X}$ for the epsilon temperature modifier (see eq. 3)	13.33
Parameter β_l for the epsilon VPD modifier (see eq. 3)	0
Parameter β_q for the epsilon VPD modifier (see eq. 3)	0
Parameter $\overline{X}$ for the epsilon VPD modifier (see eq. 3)	0.65
Average quantum efficiency (mol C (mol photon)$^{-1}$)	0.02
Parameter β_l for the epsilon leaf area index modifier (see eq. 3)	0.35
Parameter β_q for the epsilon leaf area index modifier (see eq. 3)	-0.17
Parameter $\overline{X}$ for the epsilon leaf area index modifier (see eq. 3)	5
Parameter β_l for the epsilon PAR modifier (see eq. 3)	0
Parameter β_q for the epsilon PAR modifier (see eq. 3)	0
Parameter $\overline{X}$ for the epsilon PAR modifier (see eq. 3)	1036.89
Parameter β_l for the water use efficiency - leaf area index modifier (see eq. 3)	0
Parameter β_q for the water use efficiency - leaf area index modifier (see eq. 3)	0
Parameter β_l for the water use efficiency – VPD modifier (see eq. 3)	0.78
Parameter β_q for the water use efficiency – VPD modifier (see eq. 3)	0
Average water use efficiency (mol CO_2/mol H_2O/kPa)	0
Parameter β_l for mortality model climate modifier (see eq. 3)	1.27
Parameter β_q for mortality model climate modifier (see eq. 3)	0
Parameter $\overline{X}$ for mortality model climate modifier (see eq. 3)	0.72
Parameter β_l for mean ratio of aboveground mass increment over aboveground mass (see eq. 3)	0
Parameter β_q for mean ratio of aboveground mass increment over aboveground mass (see eq. 3)	0

Ingrowth model parameters

Parameter of the relationship between the extinction coefficient and leaf area index	0.75
Parameter of the relationship between the extinction coefficient and leaf area index	-0.25
Degree days (0°C) to bud break	116.00
Degree days to end of leaf expansion	766.66
Lower base temperature for growing degree days sum	2.90
Mean foliage retention time (number of growing seasons)	10.18
Julian day when leaf fall is allowed to start (day)	270.00
Proportion of GPP partitioned to growth respiration	0.10
R_{m10} for respiration rate at 10°C	0.0106
Nitrogen concentration of foliage (gN / gC)	0.0090
Nitrogen concentration of fine roots (gN / gC)	0.0030
Nitrogen concentration of wood (gN / gC)	0.0004

Nitrogen structure roots	0.0004
Q_{10Rm} for temperature sensitivity of R_m, defined as the relative increase in respiration for a 10°C increase in temperature	2.00
R_{10} for relative increase in heterotrophic respiration for a 10°C increase in temperature (*Lloyd and Taylor*, 1994)	1.00
Heterotrophic respiration y_0 parameter (see eq. 7)	–5.252
Heterotrophic respiration *a* parameter (see eq. 7)	18.302
Heterotrophic respiration *b* parameter (see eq. 7)	0.075

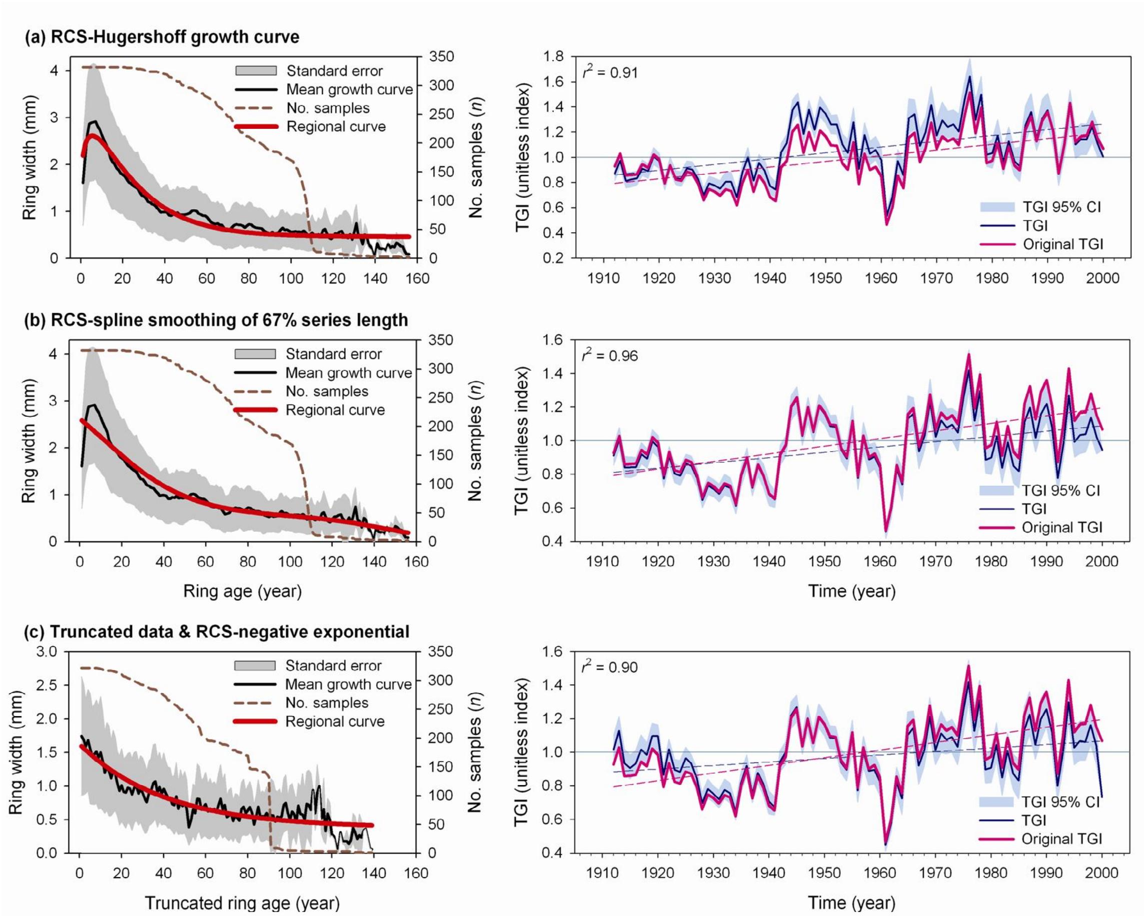

Fig. S1 Jack pine tree growth index (TGI) and 95% confidence interval (AD 1912–2000) obtained after the application of three different smoothing techniques of the mean growth curve. See Figs. 2 and 4 for definitions, and Section 4.1 for details. The original TGI used in Figs. 4 and 9 is also shown (purple curve on the right); goodness of fit between both data is indicated by the squared Pearson correlation. The final TGI record was shown to be insensitive to the use of other types of smoothing [e.g. the ‘Hugershoff’ in (a) or spline smoothing in (b)] or to truncation of the measurement series by removal of the juvenile period (first 15 to 20 years of data).

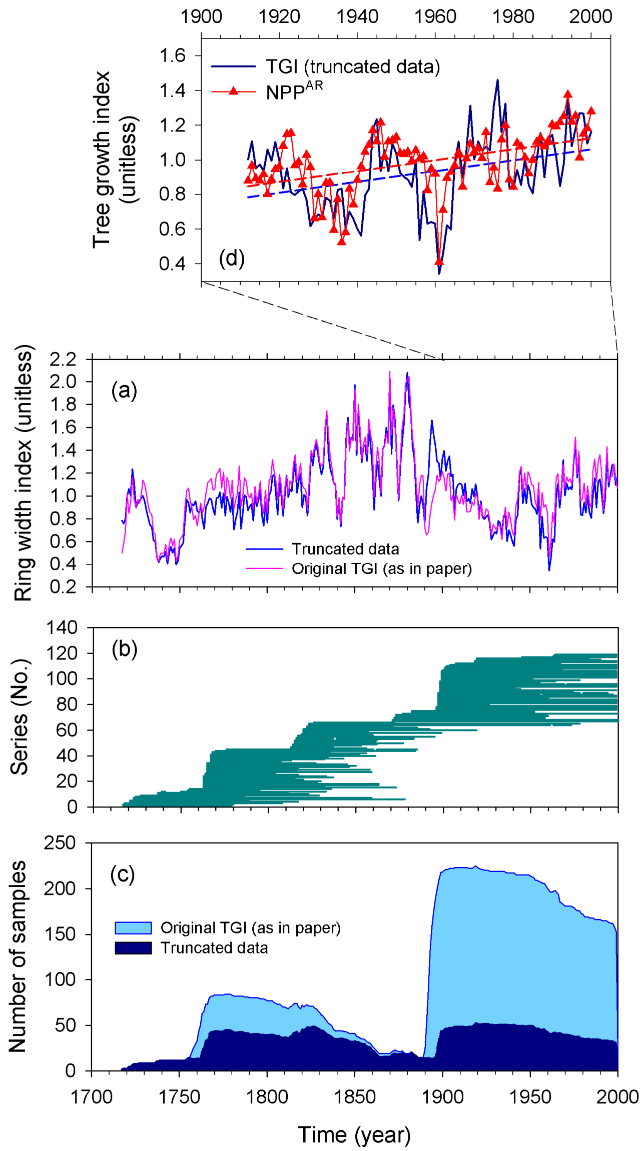

Fig. S2 Jack pine tree growth index (TGI) obtained after reducing the number of samples originating from the 1760s and 1890s age cohorts in order to meet the RCS requirement of homogeneous distribution of start and end dates. a) The final TGI chronology obtained following this data truncation versus the original chronology shown in Fig. 4a; the correlation between the two series is r = 0.91. b) Distribution of start and end dates of the truncated chronology. c) Number of tree rings used through time in both truncated data and original data (divide by 2 for an approximate number of trees). d) TGI versus the AR simulated net primary productivity (NPP^{AR}) over 1912–2000 (both are unitless indices), with linear trend lines across the data (dashed lines).

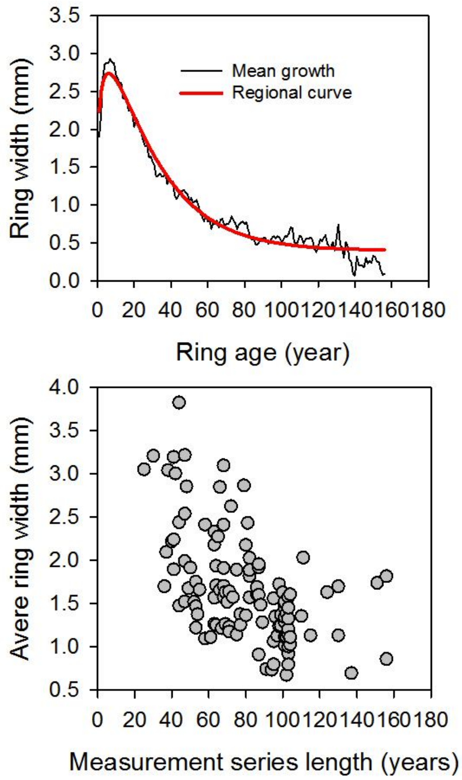

Fig. S3 Top: Regional curve used in the detrending of the jack pine ring-width measurement series (red line) obtained after reducing the number of samples originating from the 1760s and 1890s age cohorts in order to meet the RCS requirement of homogeneous distribution of start and end dates. Mean growth of trees (black line) for each ring age. **Bottom:** Relationship between average ring width and length of measurement series for each jack pine series.

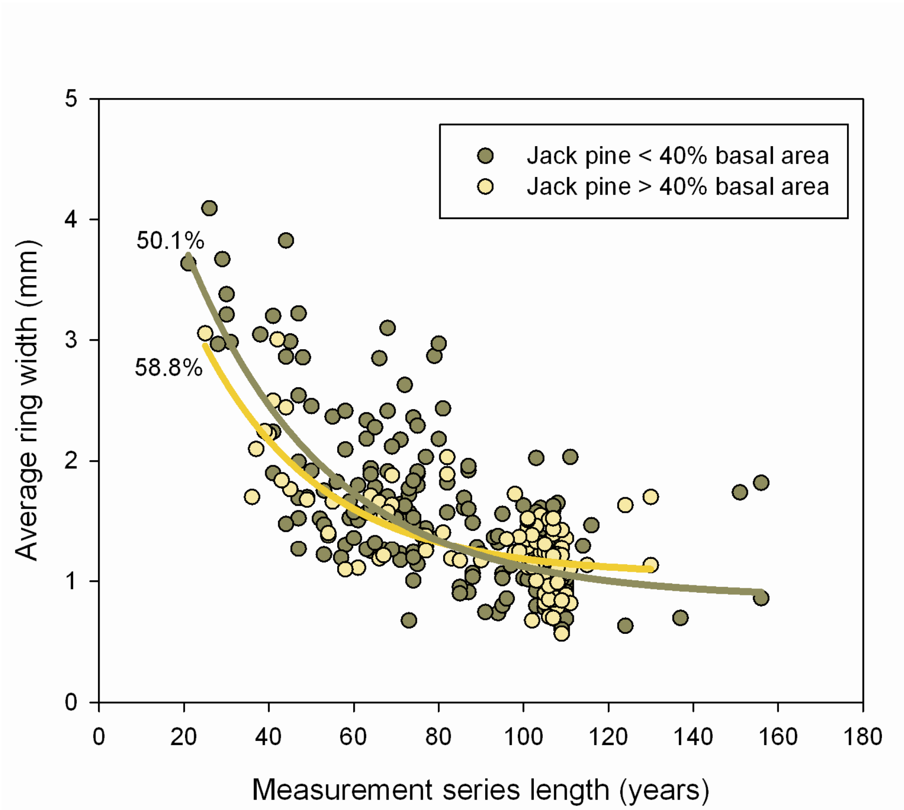

Fig. S4 Relationship between average ring width and length of measurement series for jack pine trees from forests of different cover types. The diagram differentiates between sites in which jack pine's relative basal area is above and below 40% of the total stand basal area (black spruce being most often the co-dominant species). Exponential fittings with model fits are shown. The presence of age-dependent, decreasing relationships between average tree-ring width and measurement series length suggests the existence of relatively homogeneous behaviours in the growth rates of trees, and little difference in the growth of jack pine between the stand types. A cut-off of 40% was selected to provide sufficient sample sizes in each group.

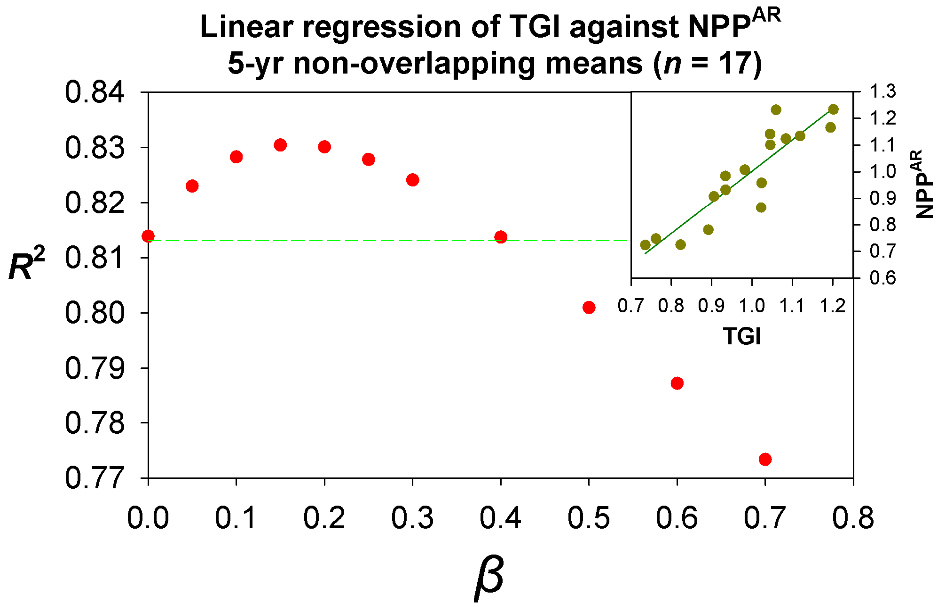

Fig. S5 *R*-squared of the least-squares linear fit between 5-yr non-overlapping means of TGI and NPP^{AR} times series (N = 17 pentads) under various simulation runs of β factors. Five-yr non-overlapping means were used instead of annual values in order to meet the normality, homoscedasticity and independence of model residuals requirements for regression analysis. 'Disconnected years' 1936 and 1976 (see text) were excluded from the calculations. The inside graph shows the scatter plot of data for the simulation run β = 0. Inclusion of a CO_2-enrichment leads to an increase in the goodness-of-fit between observed and simulated data up to β = 0.15, whereas afterwards the goodness-of-fit declines. One may note, however, that the addition of a CO_2-enrichment increases the *R*-squared by no more than 2%, which is not significant.

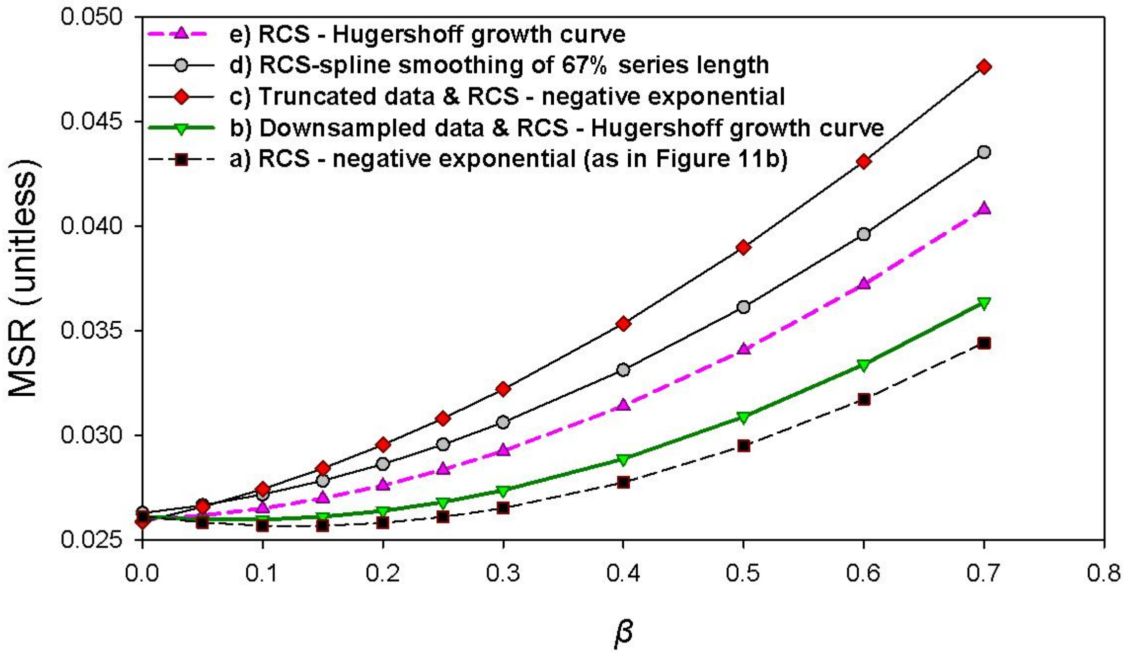

Fig. S6 The mean of squares of the residuals (MSR) of the difference between TGI and NPP^{AR}. Here, TGI series were obtained after the application of different smoothing techniques of the mean growth curve, or after data truncations of the raw measurement series (as presented in Figs. S1 and S2). When removing age-related trends in the preparation of the TGI measurement series, we used a method (RCS and exponential smoothing; see Section 4.1) that retained the most amount of trend possible. As seen here, the choice of the detrending procedure used in our analyses enhances the probability of generating false positive or Type 1 errors at lower values of β (*MSR curve a*). The use of other detrending methods would have resulted in a detection cut-off value of β much lower than 0.20 (*MSR curves b* to *e*).